

Engineering Notes

ENGINEERING NOTES are short manuscripts describing new developments or important results of a preliminary nature. These Notes cannot exceed 6 manuscript pages and 8 figures; a page of text may be substituted for a figure and vice versa. After informal review by the editors, they may be published within a few months of the date of receipt. Style requirements are the same as for regular contributions (see inside back cover).

Vortex Velocity Distributions at Large Downstream Distances

ANDREW H. LOGAN*

United Aircraft Corporation, Stratford, Conn.

Nomenclature

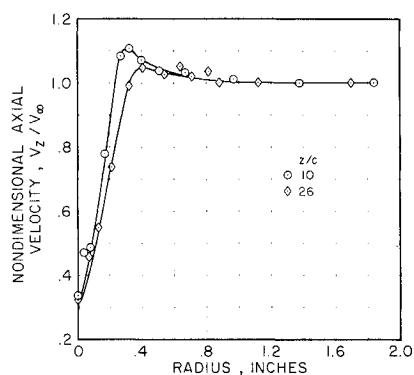
- c = midspan chord
 V_∞ = freestream velocity
 V_z = axial (streamwise) velocity
 V_θ = tangential velocity
 X, Y, Z = right-handed, orthogonal coordinate system with Z directed downstream and measured from the wing trailing edge
 α = wing angle of attack

Introduction

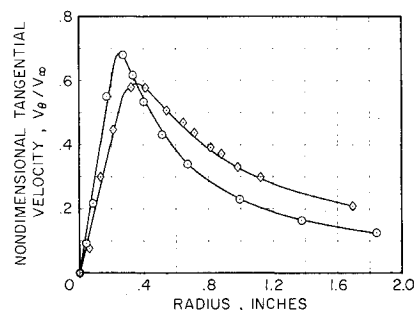
ANY wing of finite span generates a vortex sheet which is unstable and rolls up into two distinct trailing vortices within one or two chord lengths of the trailing edge. These

vortices persist after generation and may present a hazard to aircraft. The rate at which these vortices diminish, and the rate at which the hazard to aircraft diminishes, depends on the velocity structure of the trailing vortices. Most experimental investigations into the structure of the trailing vortex have been concerned with the generation and decay of the tangential velocity component.¹ However, it has been shown that the axial velocity in a trailing line vortex also will affect the persistence and decay of a vortex.² Unfortunately, the axial velocity has not been studied experimentally as extensively as the tangential velocity. Most data on the variation of the axial velocity within a vortex have been collected in connection with a study on the bursting of leading edge vortices or in a study of the near-wake vortex structure. The streamwise stations where data were collected in the study of the leading edge vortex were over a delta wing, and the trailing vortex wake was unexplored.³ In the study of the near wake, the axial, tangential and radial velocities within a trailing line vortex have been measured in close proximity to a semispan wing.⁴ Data were taken at several streamwise stations over the wing and at two and four chord lengths downstream of the trailing edge.

It is the purpose of this paper to extend the available data on the velocity structure within a trailing line vortex to large distances downstream of the generating wing. Data are presented to show the variation of both axial and tangential velocity with tunnel speed and trailing vortex strength. Specifically, data are presented at downstream distances of 10 and 26 chord lengths behind a semispan wing set at 4 and 12° angle of attack for tunnel speeds of 50 and 70 mph.



(a) AXIAL VELOCITY

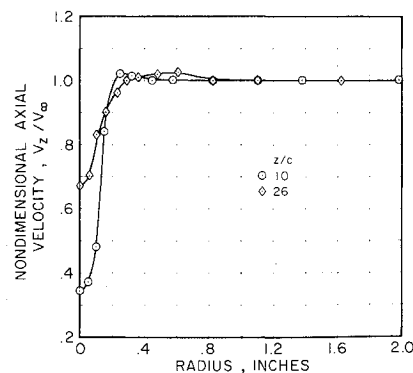


(b) TANGENTIAL VELOCITY

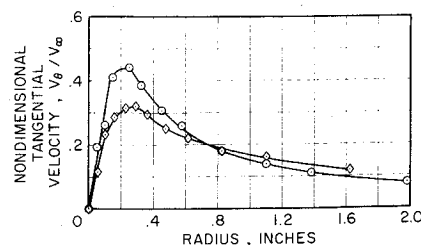
Fig. 1 Vortex velocities vs radius at two downstream stations, $V_\infty = 70$ mph, $\alpha = 12^\circ$.

Received May 8, 1971; revision received July 8, 1971. The work reported herein was done at the Pennsylvania State University and was supported by the U. S. Army Research Office (Durham) under Contract DA-31-124-ARO(D)-149. The author extends his appreciation to B. W. McCormick for his advice and encouragement.

* Research Engineer, Sikorsky Aircraft Division.



(a) AXIAL VELOCITY



(b) TANGENTIAL VELOCITY

Fig. 2 Vortex velocities vs radius at two downstream stations, $V_\infty = 70$ mph, $\alpha = 4^\circ$.

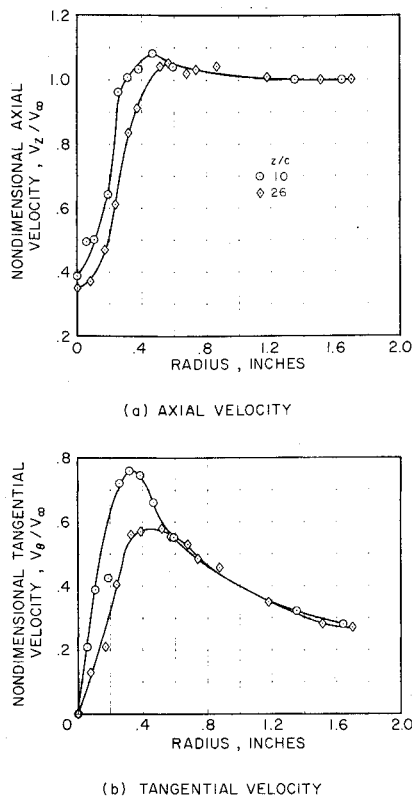


Fig. 3 Vortex velocities vs radius at two downstream stations, $V_\infty = 50$ mph, $\alpha = 12^\circ$.

Experimental Equipment and Procedure

The experimental investigation was conducted in the air tunnel of the Garfield Thomas Water Tunnel at The Pennsylvania State University. The air tunnel has a test section fifteen feet long with a four foot diameter hexagonal cross section. The trailing vortex was generated at low Reynolds number (1.5×10^5 and 2.3×10^5 based on wing chord) using a one-twelfth scale semiwing of a Piper Cherokee. Velocity profiles were mapped at two downstream stations for two tunnel velocities and two semiwing angles of attack.

The test apparatus used to collect the experimental data is described in detail in Ref. 5. Briefly, the apparatus was a five holed static pressure probe attached to a positioning structure having four degrees of freedom. Yaw and pitch angular positions were achieved by two orthogonal arcs whose centers of curvature were the end of the static pressure probe. The arcs were driven by d.c. motors and the angular position was transmitted by use of a servo-transmitter-counter combination. The angular positioning mechanism was then mounted on an X-Y traversing mechanism so that the probe could be positioned at any horizontal or vertical point in the wind tunnel.

Tests were run at two downstream stations of 10 and 26 chordlengths (52 and 137 in., respectively) aft of the trailing edge for speeds of 50 and 70 mph and angles of attack of 4 and 12° . The experimental procedure was to first locate the vortex center and then make two passes, one vertically and one horizontally, through the center of the vortex. The center of the vortex was found by setting the condition of zero pitch and yaw on the angular positioning mechanism and only using the X and Y positioning mechanism to null the probe. The passes were made by moving the angular positioning mechanism vertically, or horizontally, in increments of approximately 0.05 in. At each position, the static pressure probe was nulled in both pitch and yaw and the pressure difference between the top and centerline pressure probe was recorded. The angular positions and the pressure difference were then used to determine the axial and tangential

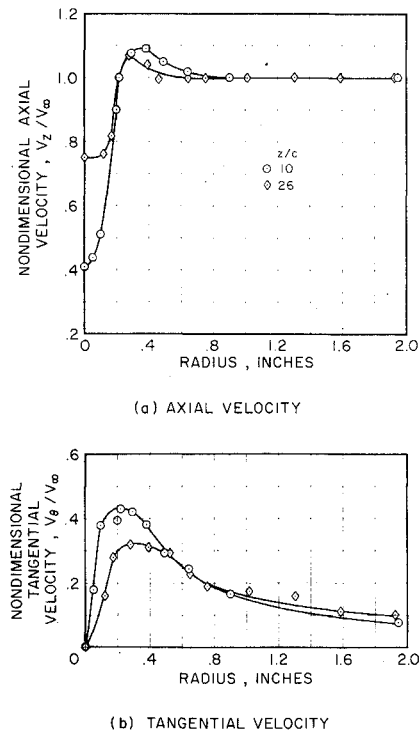


Fig. 4 Vortex velocities vs radius at two downstream stations, $V_\infty = 50$ mph, $\alpha = 4^\circ$.

velocities in the vortex. The readings from the apparatus were steady and repeatable and no trouble was encountered in positioning the probe.

Results and Discussion

The experimental data are presented in Figs. 1-4. One of the salient features of the experimental data is the significant axial velocity deficit found within the core of the trailing vortex. The deficit is shown to be as large as 65% of the freestream velocity (at $\alpha = 12^\circ$ and $V_\infty = 70$ and 50 mph) and to persist as far downstream as 26 chord lengths. For both tunnel velocities at 12° angle of attack, the axial velocity deficit remains essentially undiminished between 10 and 26 chord lengths downstream of the wing. However, at 4° angle of attack for both velocities, the axial velocity deficit has been reduced approximately 45% between the two downstream stations. An unexpected result of the experimental measurement is the appearance for all conditions tested of an axial velocity excess at the edge of the vortex core. This excess is on the order of 10% of the freestream velocity at the 10 chord lengths downstream station but decays to approximately 5% of the freestream velocity by 26 chord lengths downstream. An exact reason for this is not known.

The experimental data on the tangential velocity show that the velocity varies with radius in the classical manner; solid body rotation surrounded by a potential field. For both tunnel speeds tested, the rate of decay of the tangential velocity was greater at 4° angle of attack than at 12° . The greater rate of change at 4° angle of attack was also seen in connection with the axial velocity deficit.

Conclusions

From the experimental data collected during this study, several conclusions about the trailing vortex structure can be drawn. First, there is significant retardation of the axial velocity within the core of a trailing vortex. Second, over the downstream distance considered in this study, the axial velocity deficit will diminish for weaker vortices but remain essentially unchanged for stronger vortices. Third, for both

speeds considered, the vortex generated at 4° angle of attack dissipated more rapidly than the vortex generated at 12° angle of attack.

References

- ¹ McCormick, B. W., Tangler, J. L., and Sherrieb, H. E., "Structure of Trailing Vortices," *Journal of Aircraft*, Vol. 5, No. 3, May-June 1968, pp. 260-267.
- ² Batchelor, G. K., "Axial Flow in Trailing Line Vortices," *Journal of Fluid Mechanics*, Vol. 20, 1964, pp. 645-650.
- ³ Lambourne, N. C. and Bryer, D. W., "The Bursting of Leading-Edge Vortices—Some Observations and Discussion of the Phenomenon," R and M 3282, 1962, Aeronautical Research Council.
- ⁴ Chigier, N. A. and Corsiglia, V. R., "Tip Vortices—Velocity Distributions," presented at the 27th Annual National V/STOL Forum of the American Helicopter Society, Washington, D. C., May 1971.
- ⁵ Logan, A. H., "A Solution to the Vortex Breakdown Phenomenon in a Trailing Line Vortex," M.S. thesis, 1966 Pennsylvania State Univ., University Park, Pa.

Determining Aircraft Stability Coefficients from Dynamic Motions

S. M. BATILL* AND C. W. INGRAM†
University of Notre Dame, Notre Dame, Ind.

Nomenclature

$C_{m_\alpha}(\alpha)$	= pitching moment stability coefficient, rad^{-1}
$C_{n_\beta}(\alpha)$	= yawing moment stability coefficient, rad^{-1}
$C_{m_q} + C_{m_{\dot{\alpha}}}(\alpha)$	= pitch damping moment stability coefficient, rad^{-1}
$C_{n_r} - C_{n_{\dot{\beta}}}(\alpha)$	= yaw damping moment stability coefficient, rad^{-1}
d	= reference length, body diameter, ft
I_y	= pitching moment of inertia, slug-ft ²
I_z	= yawing moment of inertia, slug-ft ²
$M_{\delta_e \delta_e}$	= pitch trim moment, ft-lb
$N_{\delta_r \delta_r}$	= yaw trim moment, ft-lb
N	= total number of data points
Q	= dynamic pressure, slug/ft-sec ²
S	= reference area, $S = \pi d^2/4$
$SRSQ$	= sum of residuals squared
t	= time, sec
u	= magnitude of velocity, fps
α	= total angle of attack, Eq. (3)
α	= angle of attack
β	= angle of sideslip

Subscript

i = quantity evaluated at time t_i

Superscript

\wedge = denotes experimental value

Introduction

THE field of atmospheric flight dynamics has been divided into two general categories: aircraft and missile dynamics. The missile dynamicist, since he was dealing with a symmetric configuration, was able to combine the equations of motion for pitching and yawing motion to obtain the Linear Aeroballistic Theory.¹⁻² This theory yields an exact closed form solution for the position and orientation, as functions of time,

for the symmetric missile. These solutions are then fit to a missile's position and orientation data to obtain values for the aerodynamic stability coefficients for the missile. Unfortunately, the aircraft dynamicist, dealing in most cases with asymmetric configurations, has been unable to develop exact closed form solutions for the coupled differential equations of motion of pitch and yaw. The presence of inertial coupling and lack of configurational symmetry when dealing with aircraft dynamics creates a complex situation which cannot be handled by using the technique of the missile dynamicist.

Recently, a method of dynamic analysis has been developed which is a valuable aid in studying the dynamics of aircraft.³ The method involves an examination of the differential equations of motion of an aircraft system without the necessity of determining a solution to the equations of motion. By utilizing a forward numerical integration of the differential equation of motion, then fitting the integrated results to actual position data, the governing parameters, namely the stability coefficients, C_{m_α} , $C_{m_q} + C_{m_{\dot{\alpha}}}$, C_{n_β} , $C_r - C_{\dot{\beta}}$, can be determined as nonlinear functions of the total angle of attack of the configuration. This avoids the problem of imposing limiting assumptions on either the configuration or its motion in order to arrive at a closed form solution.

This Note investigates the application of this technique to the problem of the dynamics of aircraft type configurations. The method of numerical integration was analyzed using computer simulated two degree of angular freedom, pitch and yaw, motion for known values of the stability coefficients to determine the accuracy of the technique. Then two degree of freedom, subsonic wind-tunnel tests were conducted on an aircraft type configuration possessing digonal rotational symmetry to determine the nonlinear restoring and damping moment coefficients in pitch and yaw.

Numerical Integration Technique

Given an expression of the form,

$$\ddot{\alpha} = F(\alpha, \dot{\alpha}, t) \quad (1)$$

with a knowledge of the functionality F and the initial conditions on $\dot{\alpha}$ and α , it is possible to numerically integrate this equation to yield a time history of α . In dealing with the experimental dynamic motion though, usually the opposite is true. One has a time history of the dependent variable and is interested in the form of the functionality F . Models representing the form of the function F have been developed but the form and constants vary with each physical case. The numerical integration technique proposes choosing one of the various models available and then with a proper choice of initial conditions and parameters integrating the differential equation of motion Eq. (1), and comparing the integrated results with an existing set of data. This process may be repeated after correcting the parameters to improve the comparison until the integrated values fit the experimental data to a desired accuracy. Then the characteristic parameters of the chosen mathematical model have been determined for the particular set of data.

The numerical integration technique⁴ was applied to a simplified form of the equations of motion for a nonrolling aircraft type configuration in which coupling takes place in the

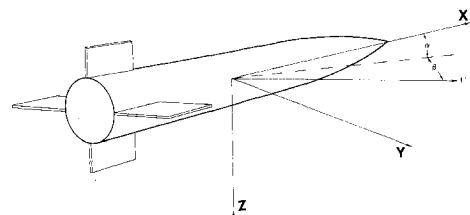


Fig. 1 Model and coordinate system.

Received July 22, 1971.

* NSF Trainee. Member AIAA.

† Assistant Professor, Aerospace and Mechanical Engineering Department. Member AIAA.